**PVDF/$BaTiO_3$/Carbon Nanotubes Ternary Nanocomposites: Effect of Nanofillers and Processing**

F.A. Sanchez, J. González-Benito*

*Dpt. Materials Science and Engineering, IQMAAB, Universidad Carlos III de Madrid. Av. Universidad 30, 28911 Leganés (Madrid-Spain).* e-mail: javid@ing.uc3m.es

*To whom all correspondences should be addressed

Address: Av. Universidad 30, 28911 Leganés (Madrid – Spain)

e-mail: javid@ing.uc3m.es

**PVDF/$BaTiO_3$/Carbon Nanotubes Ternary Nanocomposites: Effect of Nanofillers and Processing**

F.A. Sanchez, J. González-Benito*

*Dpt. Materials Science and Engineering, IQMAAB, Universidad Carlos III de Madrid. Av. Universidad 30, 28911 Leganés (Madrid-Spain).* e-mail: javid@ing.uc3m.es

**Abstract**

Ternary thermoplastic systems based on poly(vinylidene fluoride), PVDF, filled with barium titanate, $BaTiO_3$, submicrometric particles and carbon nanotubes, CNT, were prepared. Their structure and morphology were studied as a function of composition and finally correlated with thermal and mechanical properties. High energy ball milling, HEBM, under cryogenic conditions and subsequent hot pressing were used to obtain films with quite uniform dispersion of the nanofillers. The presence of $BaTiO_3$ particles and CNT did not modify the thermodegradation mechanism of the PVDF. However, enough amount of $BaTiO_3$ seemed to inhibit the volatility of the products of pyrolysis, hindering the decomposition of PVDF. The presence of CNT favored the PVDF thermodegradation probably due to improved heat transmission by an increased in the thermal conductivity. Variations in PVDF thermal transitions were more dependent of processing conditions. Improvements in the mechanical properties of PVDF were ascribed to a reinforcing effect of the fillers. This effect only happened below the fraction of percolation of CNT, pointing out that CNT reinforce through an optimum load transfer from the PVDF matrix to the nanofillers.

**Keywords:** Nanocomposites; poly(vinylidene fluoride); Barium titanate; Carbon nanotubes.

## 1. Introduction

Thermoplastic easy processing materials with high electric permittivity are receiving special attention lately. They have high potentiality to be used in electric energy storage devices, capacitors and actuators among others. However, taken into account that most of thermoplastic polymers have low permittivity their specific modification is wanted but without compromising other properties. For instance, addition of ceramic fillers with high dielectric constant seems to be the simplest way to achieve that challenge [1]. In general, significant increase of the dielectric constant can be achieved only with the use of important loads of ceramic filler (more than 40% vol) [2, 3]. However, such amount of filler might compromise other important properties for proper material performance. Therefore, other possibilities should be investigated; for instance, the addition of a third phase which allows enhancing the synergy at low loads of the ceramic filler.

Results of some groups evidenced important increase of the dielectric constant of polymers when they were loaded with conductive particles in the neighborhood of the percolation threshold [4-8]. Thus, filling polymers with a combination of high k dielectric particles (i.e. barium titanate) and conductive particles (i.e. graphene, carbon nanotubes or carbon nanofibers) would be an interesting option to increase the permittivity of polymers. In those cases it is reasonable to think that, for an appropriate dispersion of this kind of fillers, nano or microcapacitors might be formed within the polymer matrix. In fact, when the volume fraction of the conductive filler is close to the percolation threshold, an abrupt increase of the dielectric constant in the conductive filler-polymer composite can be understood by the same idea [9, 10]. In this sense, carbon nanotubes (CNT) with superior electrical and thermal conductivity values must be an excellent choice to enhance the permittivity of this kind of composites. CNTs allow much lower percolation threshold in composites than conventional spherical fillers since high-aspect ratio of the conductive fillers must facilitate the formation of conducting networks at much lower volume fraction. Besides, CNTs present extremely high mechanical strength which can prevent loss in mechanical properties of the polymer matrix due to the presence of the ceramic particles or even improve them.

Therefore, in the frame of this kind of materials it is necessary to know and understand the influence of the joint presence of different fillers in the final properties. For instance,

do changes occur due to the sole presence of the fillers or are they due to modification of the structure and/or morphology of the polymer? In fact, the addition of different kind of fillers into crystalline polymer matrices may affect apart from the conformation and the morphology, their crystalline phases, the formation of spherulites and the crystallization rate [11-15].

Because of its good piezoelectric and pyroelectric properties, Poly(vinylidene fluoride), PVDF, as a semicrystalline polymer, is being used to make sensors, actuators and transducers. Because of its good mechanical strength and high stability to moisture, chemicals, abrasions, and intense radiation this polymer has many advantages over traditional ceramic electroactive materials [16]. Although four phases, $\alpha$, $\beta$, $\gamma$ and $\delta$ [17, 18] are mainly indentified in PVDF, $\alpha$ (the most stable) and $\beta$ (the most polar showing the most important piezoelectric response) phases are the most used and studied [19, 20]. However, recently some results are pointing out that mechanical and thermal properties so as the corrosion resistance of neat PVDF do not seem to be good enough for certain requirements as those necessary in space environment [21, 22]. Hence, efforts should be focused to improve these properties apart from the electrical properties already mentioned.

CNT reinforced PVDF nanocomposites have shown improvements in mechanical, thermal, and electrical properties compared to neat PVDF [23]. Relatively recent studies about PVDF/CNT nanocomposites indicate that when adding CNT to PVDF, $\alpha$-phase to $\beta$-phase crystal transformation can be induced. Besides, CNT may act as nucleating agents of PVDF exerting a crystallization confinement that depends on its concentration [24, 25]. However, a clear origin of those changes is not revealed yet, being the answer to that question even more difficult when a second filler is incorporated within the polymer matrix.

It is generally accepted that these materials show their best performance with uniform dispersion of the filler, mainly because the presence of agglomerates may lead to non-desired electrical or mechanical properties [26]. This characteristic is particularly difficult to achieve in the case of using carbon nanotubes as the filler since they tend to be aggregated because of important Van der Waals attractions. Although there have

been a lot of strategies to achieve efficient dispersion of nanoparticles in different matrices: i) modification of the nanoparticles surface [27-29]; ii) "in situ" polymerization by prior dispersion of the nanoparticles in a monomer [30]; iii) addition of surfactants or other dispersant substances [31], etc., it has not been found any yet which ensure uniform dispersions in polymer matrices when the amount of nanofiller is higher than 5% by weight or when the polymer is highly viscous. However, using high energy ball milling promising results have been obtained [3, 11, 12, 32-34]. It seems that strong shear forces imposed by the milling process help the nanoparticles to be randomly embedded into the polymer [11].

The aim of this work is to prepare ternary nanocomposites based on PVDF filled with $BaTiO_3$ submicrometric particles and CNT with uniform dispersion of them. Structure and morphology (in terms of particle dispersion) of the nanocomposites were studied to finally correlate then with thermal and mechanical properties. Important data were given to understand if properties attained in the composites are due to the sole presence of the particles, the structure and morphology variations induced in the polymer matrix or a sum of contributions of both possibilities.

## 2. Experimental part

### *2.1. Materials*

Poly(vinylidene fluoride), PVDF, supplied by Sigma-Aldrich ($M_n$ ~ 10,700; $M_w$ ~ 27,500 and density 1.78 g/cm$^{-3}$) was used as the polymer matrix. Two types of fillers were used: i) multiwall carbon nanotubes, CNT, purchased from Sigma-Aldrich (more than 95 wt% of carbon, diameter = 6 to 9 nm, length = 5 μm and density 2.1 g/cm$^3$) and ii) barium titanate particles supplied by Nanostructred and amorphous materials (tetragonal structure, mean diameter 200 nm, 99.9 wt% of purity and density 6.02 g/cm$^3$).

### *2.2. Sample preparation*

Different mixtures of PVDF with $BaTiO_3$ and CNTs were prepared. Codes of the samples and relative amount of each component are gathered in Table 1.

Table 1.- Codes for samples prepared and relative amount of each component.

| Sample | PVDF (% wt) | $BaTiO_3$ (% wt) | CNTs (% wt) |
|---|---|---|---|
| PVDF | 100 | 0.0 | 0.0 |
| PVDF-1BT | 99.0 | 1.0 | 0.0 |
| PVDF-5BT | 95.0 | 5.0 | 0.0 |
| PVDF-10BT | 90.0 | 10.0 | 0.0 |
| PVDF-40BT | 60.0 | 40.0 | 0.0 |
| PVDF-0.1CNT | 99.9 | 0.0 | 0.1 |
| PVDF-0.5CNT | 99.5 | 0.0 | 0.5 |
| PVDF-1.0CNT | 99.0 | 0.0 | 1.0 |
| PVDF-3.0CNT | 97.0 | 0.0 | 3.0 |
| PVDF-40BT-0.1CNT | 59.9 | 40.0 | 0.1 |
| PVDF-40BT-0.5CNT | 59.5 | 40.0 | 0.5 |
| PVDF-40BT-1.0CNT | 59.0 | 40.0 | 1.0 |
| PVDF-40BT-3.0CNT | 57.0 | 40.0 | 3.0 |

Films of the ternary nanocomposites were prepared following several steps of processing:

i) PVDF pellets were grinded using a MF10 Basic Microfine miller.

ii) Using high energy ball milling, HEBM, the grinded PVDF was then blended with $BaTiO_3$ submicrometric particles and CNT in different proportions (see Table 1). The milling was carried out under cryogenic conditions in a RETSCH MM400 apparatus using a stainless steel vessel of 50 $cm^3$ and 15 stainless steel balls of 9 mm of diameter. About 7 g of mixture were introduced in the vessel and agitated at 25 Hz for 1 h using cycles of 5 min of active milling and 15 min of resting in liquid nitrogen to finally obtain a fine powder.

iii) Films of thickness ~150 μm were prepared from the milled powders by hot pressing using a Fontijne PressesTPB374 press machine. The powders were placed between two polished 10×10 $cm^2$ aluminum plates covered by anti-adherent Kapton® sheets. Then, they were heated at 200 ºC and pressed applying a load of 50 kN. Finally, the films were cut to obtain specimens for tensile tests. The dimensions of the specimens followed the standard ISO 3167:2002 (Figure 1). A photography showing the aspect of the films in the form of tensile test specimens is also shown in Figure 1.

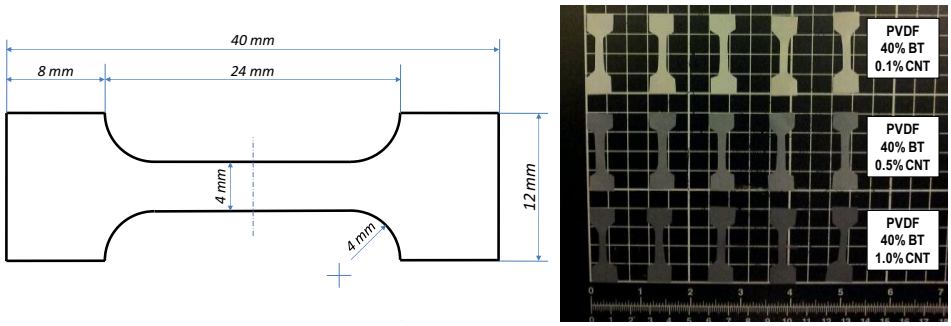


Figure 1.- Specimens of some samples under study to be subjected to tensile tests and one scheme with their dimensions.

*2.3. Equipments*

The morphology in terms of the distribution of domains with different elemental composition was imaged using a Philips XL30 scanning electron microscope, SEM, and backscattered electrons, BSE, signal. Microanalyses at specific sites on the surfaces were performed with a DX4i coupled energy-dispersive X-ray spectroscopy (EDAX) detector. To avoid charge accumulation the samples were gold coated by sputtering with a conventional anodic deposition method.

Thermogravimetric analyses were carried out in a PerkinElmer STA 6000, heating samples of about 5 mg from 50ºC to 900ºC at 10ºC/min in nitrogen atmosphere.

The melting process of PVDF matrix was dynamically analyzed by differential scanning calorimetry, DSC, in a Metler Toledo 822E. All DSC analyses were performed at 10 ºC/min under nitrogen atmosphere. In order to have information about the samples as they were processed only one heating scan from 25ºC to 210ºC at 10ºC/min without erasing thermal history was considered.

A Shimadzu Autograph Universal Testing Machine was used to perform the tensile tests. Mechanical properties (Young modulus, tensile strength, yield strength and ductility in terms of maximum deformation at break) were determined from the standard ISO 527-1:1993 and Corrigendum 1:1994). All tests were carried out pulling the specimens with a gauge length of about 28 mm. The influence of the crosshead speed was studied performing the tests at 5 and 1 mm/min respectively. Average values of the mechanical properties were obtained from the results of at least five tests corresponding to five specimens.

## 3. Results and discussion

In Figure 2 SEM images of milled PVDF with different amounts of $BaTiO_3$ are presented. The signal coming from back scattered electrons, BSE, allows distinguishing different phases in the powders since the number of scattered electrons increases with the atomic number of the elements in the samples. Due to this, $BaTiO_3$ rich domains of about 300 nm appear brighter in the images. To confirm the presence of $BaTiO_3$ in the brighter regions of the BSE images, microanalysis was performed taking the X-ray spectra of the dark and bright regions, respectively. As expected, complete lack of barium and titanium in the dark domains and clear presence of those elements in the brighter domains were observed.

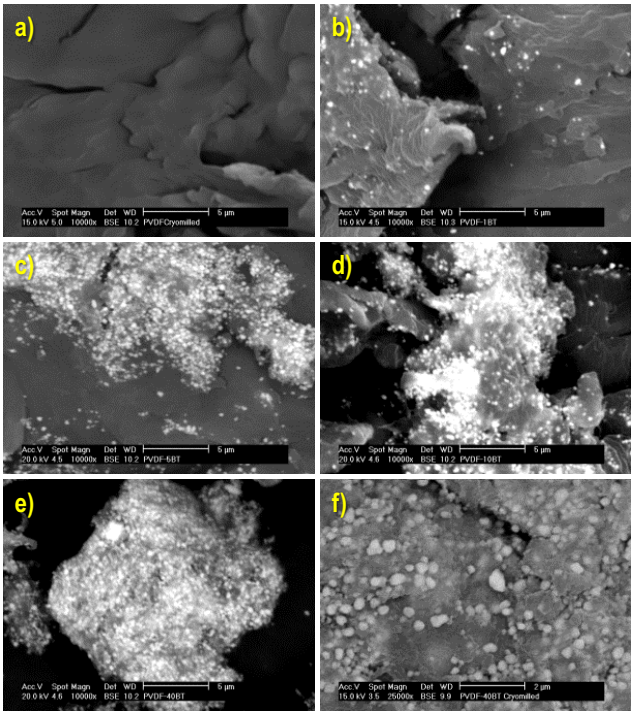


Figure 2.- BSE-SEM images of milled PVDF with different weight percents of $BaTiO_3$: a) 0%; b) 1%; c) 5%; d) 10% ; e) 40% and f) 40% (higher magnification).

Two main observations can be made from Figure 2: i) the higher amount of $BaTiO_3$ the higher number of brighter domains and ii) the milling process allows the $BaTiO_3$ particles to be uniformly dispersed within the PVDF. Figure 2f shows a higher magnification of the composite with 40 wt %. It is observed taht most of the particles are not touching each other, pointing out the uniform dispersion mentioned above. In fact, the initial morphology in form of large agglomerates of the as received particles

[33] is completely destroyed leading to isolated nanoparticles. In Figure 3 SEM images of milled PVDF with different weight percents of CNT (0%, 0.1%, 0.5% and 1%) are presented for two particular amounts of $BaTiO_3$ in the composites, 0 and 40 wt% respectively. In any case regions suggesting high accumulation of CNT were not observed. Besides, although isolated CNT cannot be seen because of the SEM resolution, their presence in the composites did not seem to alter the uniform dispersion of $BaTiO_3$ particles (Figure 3j). This result suggests a good dispersion of CNT since they should be only located between the $BaTiO_3$ particles.

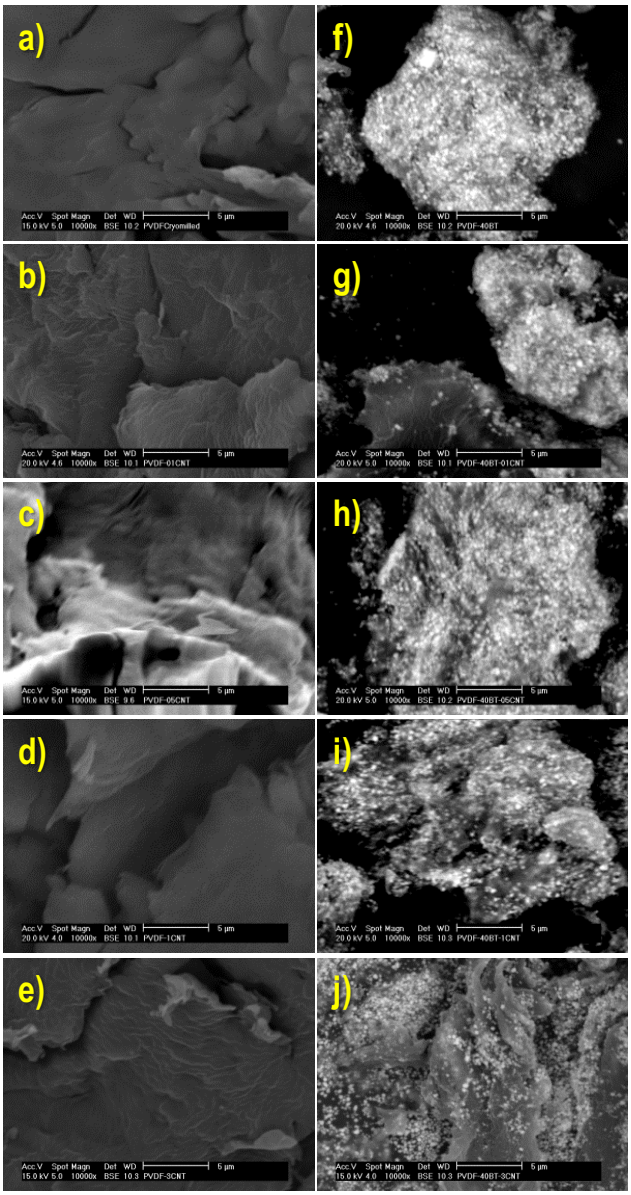


Figure 3.- BSE-SEM images of milled PVDF with different amounts of CNT for 0 weight percent of $BaTiO_3$ (0% (a); 0.1% (b); 0.5% (c); 1% (d) and 3% (e)) and 40 weight percent of $BaTiO_3$ (0% (f); 0.1% (g); 0.5% (h); 1% (i) and 3% (j)).

SEM images of the freeze fractured surfaces of the materials in the form of films were also inspected. Images at high magnification showed how the materials (after hot pressing) maintained the uniform dispersion of particles within the PVDF. However, only images at lower magnification are presented here (Figure 4) trying to show the general effect of fillers on the freeze fracture of the specimens.

In general, when $BaTiO_3$ content increases, more heterogeneous freeze fractured surfaces films are evidenced displaying more cleavage facets (Figure 4) which suggests more brittle fracture. Besides, when only CNT are added, at least for contains lower than 1 wt%, more heterogeneous freeze fractured surface is also observed pointing out more brittle fracture than that of the neat PVDF. However, in terms of freeze fracture, the effect given by the presence of $BaTiO_3$ seems to be sharper than the presence of CNT, at least when its composition is lower than 1% by weight.

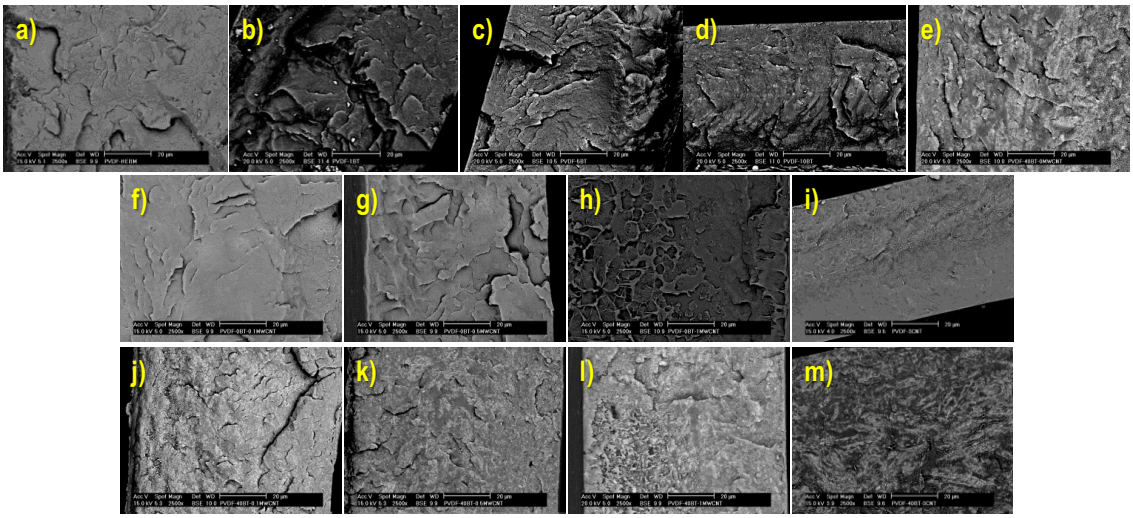


Figure 4.- SEM images of the freeze fractured surfaces of the films of all materials under study: a) PVDF; b) PVDF-1BT; c) PVDF-5BT; d) PVDF-10BT; e) PVDF-40BT; f) PVDF-0.1CNT; g) PVDF-0.5CNT; h) PVDF-1.0CNT; i) PVDF-3.0CNT; j) PVDF-40BT-0.1CNT; k) PVDF-40BT-0.5CNT; l) PVDF-40BT-1.0CNT and m) PVDF-40BT-3.0CNT.

The influence of the presence of nanoparticles and their mixtures on the thermal stability of PVDF was studied by TGA. In Figure 5 the plots of weight loss (top) and the corresponding derivates (bottom) are shown for all the samples under study. When the amount of BT increases at least until 5 wt% a slight decrease in temperature of the maximum rate of thermal degradation, $T_{max}$, is observed while above that percentage it

rises up (Table 2). In fact, there is only a considerable increase in $T_{max}$ when the amount of BT particles is 40% (Figure 5, Table 2). On the other hand, the presence of CNT decreases $T_{max}$ of the PVDF (Figure 5 and Table 2).

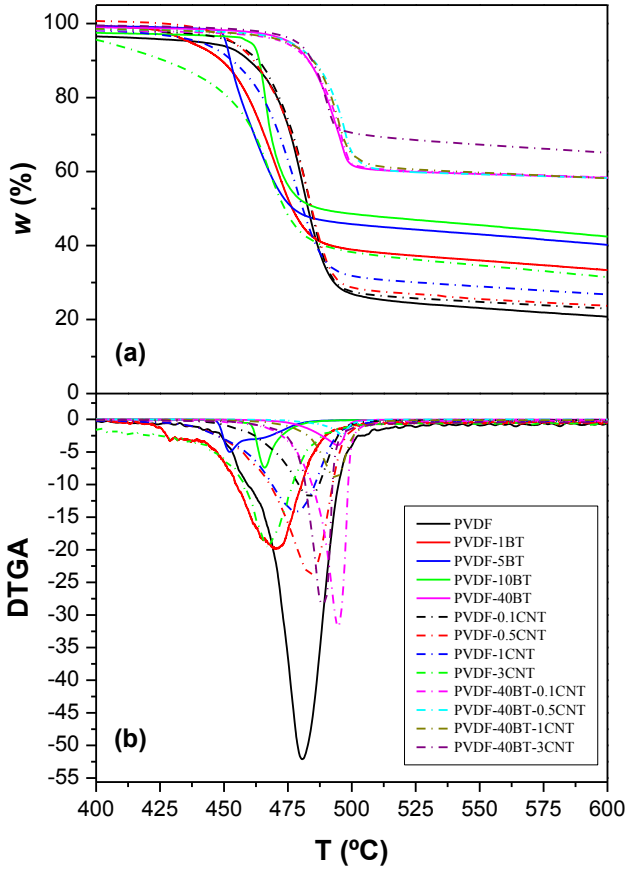


Figure 5.- Thermogravimetric analyses (a) and the corresponding derivates (b) for all the samples under study.

Table 2.- Temperatures of the maximum rate of thermal degradation for all the samples under study obtained from minima of the Figure 10b.

| **Sample** | **$T_{max}$ (ºC)** |
|---|---|
| PVDF | 481 |
| PVDF-1BT | 470 |
| PVDF-5BT | 452 |
| PVDF-10BT | 466 |
| PVDF-40BT | 495 |
| PVDF-0.1CNT | 484 |
| PVDF-0.5CNT | 484 |

| | |
|---|---|
| PVDF-1.0CNT | 478 |
| PVDF-3.0CNT | 467 |
| PVDF-40BT-0.1CNT | 495 |
| PVDF-40BT-0.5CNT | 496 |
| PVDF-40BT-1.0CNT | 494 |
| PVDF-40BT-3.0CNT | 488 |

It is usually accepted that the interaction between inorganic fillers and a polymer matrix in a composite can be explored by the effect of the fillers on the thermal degradation of the polymer. For the thermal degradation of all the samples under study a single step, similar to that observed in pure PVDF polymer, was observed (Figure 5). These results point out that the presence of nanoparticles ($BaTiO_3$ and CNT) does not modify the thermodegradation mechanism, at least under the conditions of the study.

Mendes et al. [35], studding the thermodegradation process of PVDF/$BaTiO_3$ composites observed a shift of the onset of the degradation process to higher temperatures when the amount of BT particles increased. They stated that the improvement in the stability of the polymer chains against thermal degradation should be attributed to their interaction with the ceramic filler. However, considering that as the main reason, an increase of $T_{max}$, although slight, should have been observed even at low loads of BT. Therefore, other reasons seems to be more plausible. The improvement against the thermodegradation under the presence of enough amounts of ceramic nanofiller as it happens for 40% wt of $BaTiO_3$ may be explained as Rui Song et al. did for PVDF/silica nanoparticles composites [36]. They proposed that silica nanoparticles strongly hinder the volatility of decomposed products obtained from pyrolysis, limiting therefore the continuous decomposition of PVDF content. Other possibility to explain the results obtained may be associated to the necessity of enough ceramic particles to act effectively as thermal shielding. On the other hand, the enhanced thermodegradation effect under the presence of CNT may be due to an improvement of thermal conductivity since CNT favor the heat transmission to the polymer chains. In fact the highest decrease in $T_{max}$ occurs when the concentration of CNT is above the percolation threshold for which a sharp increase in thermal conductivity should occur.

The DSC scans of all the samples under studied for which the thermal history was not erased are shown in Figure 6. Only one endothermic peak at about 168 ºC is observed in every case, being slightly shifted to higher temperature when any of the fillers was added to the PVDF. In principle, when different crystalline phases appear in polymers multiple peaks are expected from their fusion. Thus, the small shifts observed in the melting temperature seem to be due to changes in the morphology more than variations in the contribution of different crystalline phases. It is interesting to highlight here that the samples PVDF, PVDF-1BT, PVDF-5BT and PVDF-10BT were already studied by DSC giving apparently different results [12]. In that case the first DSC scan yielded two endothermic peaks, one at about 164 ºC and the other at about 167 ºC. The unique difference between the samples of reference 12 and the films of the present work was the hot pressing process used in each case. It seems therefore evident that, at least for the samples under consideration, the first DSC scan is giving information about the effect of temperature and pressure of processing. It can be concluded that the small alterations observed depend on processing conditions, influenced in addition by the presence of nanofillers, more than to specific interactions between the polymer and the nanoparticles. This result is particularly important since many times it is believed that the sole presence of some fillers alter significantly the structure and morphology of PVDF due to specific interactions. However, the main cause of those alterations might come from the way the polymer chains are arranged as a function of macromolecular dynamics which in turns depends on temperature, pressure and confinement effects (presence of fillers).

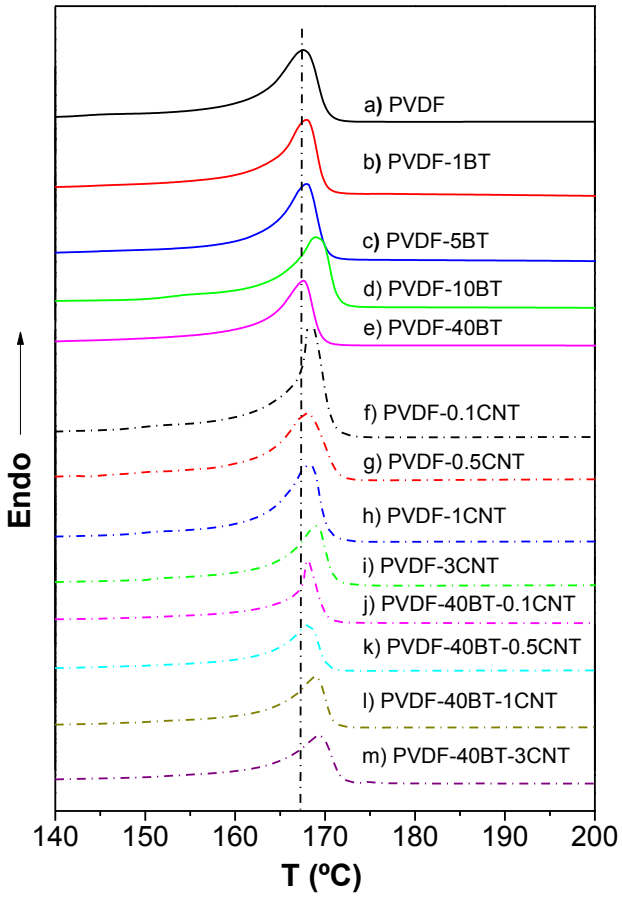


Figure 6.- DSC scans without erasing thermal history of all the samples under studied.

The influence of the presence of $BaTiO_3$ and CNT nanofillers in the mechanical properties of PVDF was explored by strain-stress tests at two different crosshead speeds. As an example strain-stress plots of all the samples under study obtained at 5 mm/min are shown in Figure 7 (similar plots were obtained for the tests performed at 1 mm/min). As can be observed the addition of particles highly reduces PVDF yielding being the effect enhanced when CNT form part of the filler.

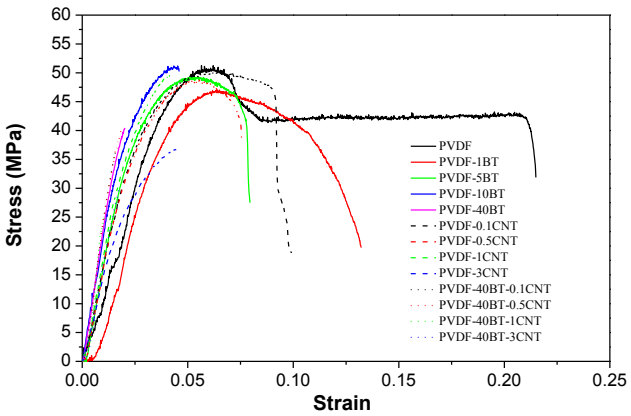

Figure 7.- Examples of strain-stress plots for all the samples under study obtained at 5 mm/min.

The main mechanical parameters are represented in Figure 8 as a function of the type of sample. Films of PVDF composites had comparable mechanical properties than those reported in literature [20, 37-39]. Without taking into account the error, it is possible to see general trends in the results obtained. When the amount of BT particles increases there is almost a linear increase in the Young's Modulus. However, it seems that there is only a stiffness increase (higher modulus) when CNT content increases, either for 0 or 40 weight percent of BT, below the percolation threshold (usually found between 2 wt% and 3 wt% of multiwall carbon nanotubes [40]). Besides, the effect of CNT on the stiffness of the composites is stronger than that of the BT particles. The enhancement of the elastic modulus with low CNT concentration, below the fraction of percolation, indicates reinforcing effect of the CNT in the PVDF/CNTs composites through the load transfer from PVDF matrix to CNT. This should be attributed to the uniform dispersion of CNTs and the good adhesion between PVDF and CNTs. However, when the percolation composition is exceeded the interconnection points between CNT might not allow transmitting efficiently loads between the components of the nanocomposite reducing the Young's modulus. On the other hand, when the rate of the tests is higher the later effect is slightly enhanced as expected for viscoelastic systems.

The mechanical strength remains nearly constant when the content of filler is relatively low (less than 10%), however for 40% of BT there is a decrease of about 20% in this parameter, being even worse as the amount of CNT increases (middle part of Figure 8). One of the main reasons may be the appearance of some aggregates or even agglomerates when the amount of nanofiller is high enough. In that case the number of interface imperfections (voids for instance) due to bad filler to polymer matrix adhesion would be higher being the cause of poor load transmission, points of stress accumulation and subsequent origin of new crack. Finally, in terms of deformation at break it is observed there is an important decrease as the amount of filler increases being more intense this effect when CNT form part of the filler. Finally, toughness (represented in this case by the relative strain at break) showed progressive drop with the increase of CNT concentration. This could be because CNT with a remarkably high

surface area restrict molecular motion of PVDF and, therefore, provide more resistance to its deformation which consequently makes the composites more brittle.

These results are in accordance with those obtained by Qin Zhang et al [38] who reported that the appropriate addition of CNT (up to 3.0 wt%) to PVDF can significantly increase its elastic modulus while decrease its fracture toughness.

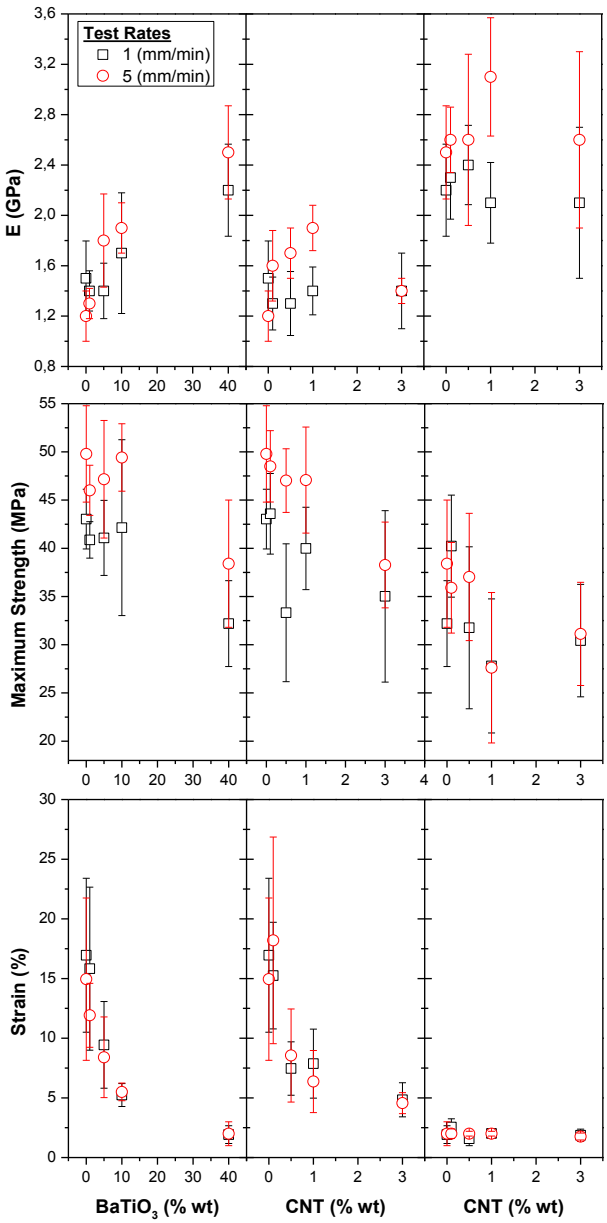


Figure 8.- Values of several mechanical parameters as a function of the kind of sample and the test rates.

In general, the modulus and strength of crystalline polymers increase with the degree of crystallinity, $\chi_c$. According to the values of $\chi_c$ obtained from the integration of DSC melting peaks, the crystallinity of PVDF does not show any significant variation with the composition of the PVDF/$BaTiO_3$/CNT composites. Therefore, improvements in modulus and strength should not be attributed to the change in crystallinty. Thus, the relevant improvements in modulus and yield strength of PVDF clearly confirm the reinforcing effect of the $BaTiO_2$ and CNTs in the PVDF/$BaTiO_3$; PVDF/CNT and PVDF/$BaTiO_3$/CNT composites.

## 4. Conclusion

High energy ball milling under cryogenic conditions allowed dispersing uniformly $BaTiO_3$ nanoparticles and CNT within PVDF. A filler formed by $BaTiO_3$ nanoaprticles or/and CNT did not modify the PVDF thermodegradation mechanism at least under the studied conditions. However: i) $BaTiO_3$ seems to hinder the volatility of the decomposed products obtained from pyrolysis of PVDF limiting its continuous decomposition and ii) CNT must increase thermal conductivity of the composites enhancing their thermodegradation. Variations in PVDF thermal transitions are more dependent on processing conditions, influenced by the presence of nanofillers, than to exclusively specific interactions between the polymer and the nanoparticles. Significant improvements in modulus and yield strength of PVDF clearly confirm the reinforcing effect of the $BaTiO_3$ and CNT in the PVDF/$BaTiO_3$; PVDF/CNT and PVDF/$BaTiO_3$/CNT composites only below the CNT fraction of percolation, pointing out that CNT reinforce the polymer matrix through an effective load transfer from PVDF to CNT.

**Acknowledgments**

Authors gratefully acknowledge financial support of the Ministerio de Ciencia e Innovación (MAT2010-16815).

## 5. References

1. P. Barber, S. Balasubramanian, Y. Anguchamy, S. Gong, A. Wibowo, H. Gao, H. J. Ploehn, H Loye, *Materials*, **2**, 1697 (2009).
2. Y. Bai, Z. Y. Cheng, V. Bharti, H. S. Xu, Q. M. Zhang, *Appl. Phys. Lett.*, **76**, 3804 (2000).

3. D. Olmos, J. M. Martínez-Tarifa, G. González-Gaitano, J. González-Benito, *Polym. Test.*, **31**, 1121 (2012).
4. Q.K. Guo, Q.Z. Xue, J. Sun, M.D. Dong, F.J. Xia, Z.Y. Zhang, *Nanoscale*, **7**, 3660 (2015).
5. Z. M. Dang, L. Z. Fan, Y. Shen, C. W. Nan, *Chem. Phys. Lett.*, **369**, 95 (2003).
6. S. H. Yao, Z. M. Dang, M. J. Jiang, J. B. Bai, *Appl. Phys. Lett.*, **93**, 182905 (2008).
7. Z.M. Dang, J. K. Yuan, J. W. Zha, T. Zhou, S. T. Li, G. H. Hu, *Prog. Mat. Sci.*, **57**, 660 (2012).
8. F. Chiu, Y. Chen, *Composites: Part A*, **68**, 62 (2015).
9. C. Pecharroman, J. S. Moya, *Adv. Mater.*, **12**, 294 (2000).
10. Z.M. Dang, S. H. Yao, J. K. Yuan, J. Bai, *J. Phys. Chem. C*, **114**, 13204 (2010).
11. D. Olmos, C. Domínguez, P. D. Castrillo, J. González-Benito, *Polymer*, **50**, 1732 (2009).
12. D. Olmos, F. Montero, G. Gonzalez-Gaitano, J. Gonzalez-Benito, *Polym. Comp.*, **12**, 2094 (2013).
13. F. Chiu, *Mater. Chem. Phys.*, **143**, 681 (2014).
14. J. T. Feng, J. H. Sui, W. Cai, J. Q. Wan, A. N. Chakoli, A. Nabipour; Z. Y. Gao, *Mater. Sci. Eng. B*, **150**, 208 (2008).
15. Y. Xu, W. T. Zheng, W. Xe. Yu, L. G. Hua, Y. J. Zhang, Z. D. Zhao, *Chem. Hem. Res. Chin. Univ.*, **26**, 491, (2010).
16. Q. X. Chen, P. A. Payne, *Meas. Sci. Technol.*, **6**, 249 (1995).
17. P. Martins, A.C. Lopes, S. Lanceros-Mendez, *Prog. Polym. Sci.*, **39**, 683 (2014).
18. R. Gregorio, R. C. Capitao, *J. Mater. Sci.*, **35**, 299 (2000).
19. R. Jr. Gregorio, D. S. Borges, *Polymer*, **49**, 4009 (2008).
20. J. S. Nunes, A. Wu, J. Gomes, V. Sencadas, P. M. Vilarinho, S. Lanceros-Méndez, *Appl. Phys. A*, **95**, 875 (2009).
21. J. Gomes, J. S. Nunes, V. Sencadas, S. Lanceros-Mendez, *Smart Mater. Struct.*, **19**, 065010 (2010).
22. E. Grossman, I. Gouzman, *Nucl. Instrum. Methods Phys. Res.*, **208**, 48 (2003).
23. I. Kim, D.H. Baik, Y.G. Jeong, *Macromol. Res.*, **20**, 920 (2012).
24. L. He, J. Sun, X. Zheng, Q. Xu, R. Song, *J. Appl. Polym. Sci.*, **119**, 1905 (2011).
25. C. Tang, B. Li, L. Sun, B. Lively, W. Zhong, *Eur. Polym. J.*, **48**, 1062 (2012).
26. L. He, X. Zheng, Q. Xu, *J. Phys. Chem. B*, **114**, 5257 (2010).
27. D. Tan, Y. Cao, E. Tuncer, P. Irwin, *Mater. Sci. Applications*, **4**, 6 (2013).

28. P. Kim, S. C. Jones, P. J. Hotchkiss, J. N. Haddock, B. Kippelen, S. R. Marder, J. W. Perry, *Adv. Mater.*, **9**, 1001 (2007).
29. M. J. Yang, Y. Dan, *Colloid Polym. Sci.*, **84**, 243 (2005).
30. B. J. Ash, R. W. Siegel, L. S. Schadler, *Macromolecules*, **37**, 1358 (2004).
31. D. N. Bikiaris, A. Vassiliou, E. Pavlidou, G. P. Karayannidis, *Eur. Polym. J.*, **41**, 1965 (2005).
32. E. Reynaud, T. Jouen, C. Gauthier, G. Vigier, J. Varlet, *Polymer*, **42**, 8759 (2001).
33. P. D. Castrillo, D. Olmos, D. R. Amador, J. González-Benito, *J. Colloid Inter. Sci.*, **308**, 318 (2007).
34. R. Serra, G. Gonzalez-Gaitano, J. González-Benito, *Polym. Compos.*, **33**, 1549 (2012).
35. D. Olmos, E. Rodríguez-Gutiérrez, J. González-Benito, *Polym. Compos.*, **33**, 2009 (2012).
36. S.F. Mendes, C.M. Costa, C. Caparros, V. Sencadas, S. Lanceros-Méndez, *J. Mater. Sci.*, **47,** 1378 (2012).
37. R. Song, D. Yang, L. He, *J. Mater. Sci.*, **42**, 8408 (2007).
38. Q. Zhang, R. Adebisi, J. Gladden, *Polym. Compos.*, **33**, 509 (2012).
39. C. Yu, D. Li, W. Wu, C. Luo, Y. Zhang, C. Pan, *J. Mater. Sci.*, **49**, 8311 (2014).
40. C. M. Chang, Y. Liu, *Carbon*, **48**, 1289 (2010).